Evidence for Lipid-Dependent Structural Changes in Specific Domains of Apolipoprotein B100[†]

Vinita Chauhan, Xingyu Wang, Tanya Ramsamy, Ross W. Milne,* and Daniel L. Sparks*

Lipoprotein and Atherosclerosis Group, University of Ottawa Heart Institute, 1053 Carling Avenue, Ottawa, Ontario, Canada K1Y 4E9

Received August 1, 1997; Revised Manuscript Received January 7, 1998

ABSTRACT: The structural organization and stability of apoB100 in complexes containing triglyceride (TG) and phospholipid have been examined. LDL was delipidated to form aqueous soluble apoB100−TG complexes that retain ∼70% of LDL TG, but contain no other lipids. The apoB100−TG complexes exhibited reduced amphipathic α-helical content (17%) and net negative charge (−2.9 mV) as compared to native LDL−apoB100 (49% and −6 mV, respectively). Of 28 anti-apoB monoclonal antibodies tested, 15 showed partial or full reactivity with apoB100−TG. The immunoreactive epitopes of apoB100−TG were restricted to those situated in either the amino terminal globular domain (4 of 6) or in regions of apoB100 that are predicted to be composed of amphipathic β-strands (11 of 13). Incubation of the apoB100−TG complex with palmitoyloleoylphosphatidylcholine (POPC) spontaneously (<10 min) formed homogeneous lipoproteins (20 nm) that contained approximately 300 molecules of POPC per particle (apoB100−PC). Phospholipidation of apoB100−TG complexes partially recovered the α-helical content (34%) and net negative charge (−4.9 mV) of the native LDL and restored resistance of apoB100 to denaturation by guanidine HCl (5.8 M). Addition of phospholipids to apoB100−TG also increased the immunoreactivity of specific epitopes that are located primarily in regions of apoB100 that are thought to be constituted of amphipathic β-strands. The effects of TG and phospholipid on apoB100 conformation appear to be highly domain-specific. On the basis of these results, we propose that the β-strands of apoB100 may represent a nonflexible lipid-associating backbone, while the amphipathic α-helical domains may represent flexible lipid-binding regions that allow the particle to accommodate varying amounts of lipid.

Human apolipoprotein B100 (apoB100) is a very large amphipathic protein that is necessary for the hepatic assembly of triglyceride-rich lipoproteins (*1*). It is composed of 4536 amino acids and is synthesized in hepatocytes and secreted primarily in the form of very low density lipoproteins (VLDL). Immuno-electron microscopy suggests that, on low-density lipoproteins (LDL), apoB100 adopts an extended structure that wraps around the spherical particle (*2*, *3*). The regions of apoB that are responsible for lipid binding are nonrandomly distributed within its primary structure (*4*). On the basis of the identification of apoB fragments that were either released from or remained with LDL particles following trypsin digestion, Yang et al. (*5*) have proposed that apoB100 is composed of five domains that differ in their relative affinities for lipid and/or trypsin accessibility. Segrest et al. (*6*) have proposed a similar pentapartite model for apoB secondary structure following a computer-assisted analysis of apoB primary structure. In this model, apoB would be composed of five domains: an amino terminal domain that would have a globular structure and include a cluster of amphipathic α-helixes (α_1 domain) with relatively low affinity for lipid, two domains enriched in amphipathic β-sheets that would bind lipid irreversibly (β_1 and β_2 domains), and two domains composed of amphipathic α-helixes that would strongly, but reversibly, bind lipid (α_2 and α_3 domains). According to this model, the predicted domain organization for apoB100 was $\alpha_1-\beta_1-\alpha_2-\beta_2-\alpha_3$. It is unclear how these various domains of apoB100 act in concert to promote the formation of a VLDL particle during the various stages of lipoprotein assembly. However, on the basis of studies in which short fragments of human apoB were expressed in rat hepatoma cells as apoA-I−apoB fusion proteins, it has been proposed that specific sequences within regions predicted to have an amphipathic β-structure in the amino terminal half of apoB are responsible for the recruitment of TG into hepatic VLDL particles (*7*).

In the present work, we have attempted to characterize the effect of the progressive lipidation of apoB100 on its structural properties and on the conformation of specific domains within this protein. We describe the physicochemical and immunochemical properties of an apoB100−TG complex derived from cholate delipidated native LDL and the effect of phosphatidylcholine on the conformation and stability of apoB100. On the basis of our results, we present

[†] This work was supported by Medical Research Council Grant PG-11471.

* Authors to whom correspondence should be addressed.

[1] Abbreviations: apo, apolipoprotein; BSA, bovine serum albumin; CE, cholesteryl ester; DMPC, dimyristoylphosphatidylcholine; POPC, 1-palmitoyl-2-oleoylphosphatidylcholine; GGE, gradient gel electrophoresis; GdnHCl, guanidine HCl; LDL, low-density lipoprotein(s); mAb, monoclonal antibody; NaDOC, sodium deoxycholate; PBS, phosphate-buffered saline; RIA, radioimmunoassay; TG, triacylglycerol; VLDL, very low density lipoprotein(s).

S0006-2960(97)01885-0 CCC: $15.00
Published on Web 02/25/1998

a functional model of apoB secondary structure in which the amphipathic β domains are intimately associated with the neutral lipid core and serve as a rigid backbone of the molecule, whereas the amphiphathic α-helical domains are flexible and allow for the changes in particle size and composition that occur during assembly and intravascular metabolism.

EXPERIMENTAL PROCEDURES

Chemicals. 1-Palmitoyl-2-oleoylphosphatidylcholine, dimyristoylphosphatidylcholine, and guanidine HCl (GdnHCl) were obtained form Avanti Polar Lipids (Birmingham, AL) and Bethesda Research Laboratories (Bethesda, MD). All other reagents were analytical grade.

Delipidation of LDL with Sodium Deoxycholate. LDL (d = 1.019−1.063 g/mL) was isolated from fresh plasma of normolipidemic donors by sequential ultracentrifugation (*8*). ApoB100 was isolated from LDL using a delipidation procedure similar to that described previously (*9*). LDL was dialyzed against 50 mM NaCl and 50 mM Na_2CO_3 (pH 10) overnight and then incubated with NaDOC at a weight ratio of 1:12 (apoB100:cholate) for 30 min in the dark at room temperature. After incubation, the solubilized protein (clear yellow solution) was separated from lipid and detergent by gel filtration on a Sepharose CL-4B column (1.6 cm × 60 cm). The column was equilibrated with 35 mM NaDOC and 50 mM Na_2CO_3 (pH 10). The apoB100 protein was eluted with 50 mM NaCl, 50 mM Na_2CO_3, and 10 mM NaDOC (pH 10, 4 °C) in the void volume with a recovery of approximately 74%. To remove excess bile salt and detergent, fractions containing apoB100 were chromatographed on a Sephadex G-75 column (1.6 cm × 30 cm) and eluted with 0.01 M Tris-HCl buffer, pH 9. The apoB100 protein eluted in the void volume as a clear solution with a recovery of 85%, while the bile salts eluted close to the total bed volume of the column. Fractions were collected and analyzed for protein and lipid compositions after each separation step. The isolated apoB100 samples contained less than 0.04 molecule of NaDOC per molecule of apoB100 after gel filtration on Sephadex G-75, as determined by electrophoresis (0.5% agarose gel) of apoB100 in the presence of known amounts of NaDOC.

Determination of Physical and Structural Characteristics of ApoB100−Lipid Complexes. The size and homogeneity of the apoB100 complexes were estimated by electrophoresis on a 4−15% gradient gel under nondenaturing conditions (*10*). The surface charge characteristics of lipoprotein particles were determined from electrophoretic mobility by electrophoresis on 0.5% agarose gels at pH 8.6 (*11*). Total and free cholesterol and phosphatidylcholine contents were determined enzymatically using Boehringer Mannheim (Indianapolis, IN) kits according to manufacturer's procedures. Phospholipids were also determined by phosphorus assay (*12*), and proteins were determined by the modified Lowry method (*13*).

Association of ApoB100 with Phosphatidylcholine. The ability of apoB100−TG to associate with DMPC and POPC was determined by a turbidity clearance assay. The desired amount of phospholipid was dried to completion under nitrogen and solubilized in Tris buffer (1 mg/mL). Before the assay, POPC and apoB100−TG samples (at molar ratio of 100:1 or 300:1) were preincubated independently at the desired temperature (from 4 to 24 °C) for 10 min. The lipid and protein were combined, and the rate of lipid−protein association was followed by monitoring the reduction in turbidity at 325 nm. After complexation of POPC with apoB100−TG, the samples were separated from free lipids by chromatography on a Superose-6 gel filtration column. The POPC-to-apoB ratio in the resulting particle was determined by phosphorus and protein assays as described above.

Determination of Secondary Structure and Stability of ApoB100. The average secondary structures of apoB100 were monitored by CD spectroscopy on a Jasco J41A spectropolarimeter calibrated with a 0.1% (w/v) D-10-camphorsulfonic acid solution (*14*). CD spectra were measured at 24 °C at a 0.1 cm path length quartz cell, and eight scans from 260 to 184 nm were collected and averaged. The percent α-helix in apoB100 was calculated from the molar ellipticity at 222 nm using a mean residue weight of 112.9. The effect of GdnHCl concentration on the secondary structure of apoB100 was monitored by the changes in molar ellipticity at 222 nm. Aliquots of each lipoprotein sample (33 μg of protein/mL of buffer) were incubated with different concentrations of GdnHCl (ranging from 0 to 6 M) in 0.l05 M phosphate buffer (pH 7.2, 4 °C) for 72 h.

Immunoreactivity of ApoB100 with Monoclonal Antibodies. Immulon II Removawells (Dynatech Laboratories, Chantilly, VA) were coated with 200 μL of reference LDL (30 μg/mL, 5 mM glycine, pH 9.2) overnight and subsequently saturated by incubations for 1 h with 250 μL of 1% bovine serum albumin (BSA) in phosphate-buffered saline (PBS), pH 7.4. Serial dilution (125 μL) of test and control LDL were prepared, and 125 μL of monoclonal antibody (mAb), appropriately diluted in PBS containing 1% BSA, was added to the diluted LDL and allowed to incubate for 4 h at room temperature. Aliquots (200 μL) of the LDL/mAb mixture were transferred to the LDL-coated Removawells that had been washed with 0.15 M NaCl containing 0.025% Tween 20 (Tween-saline). The wells were incubated overnight and washed with Tween-saline as above and counted for bound radioactivity (*15*). Most of the anti-apoB mAbs have been characterized previously (*15*−*17*).

LDL Receptor Binding. The ability of test lipoproteins to compete with ^{125}I-LDL for binding to the LDL receptor on cultured human fibroblasts was determined as previously described (*15*). ^{125}I-LDL was prepared by the iodine monochloride method (*18*).

Mathematical Analysis. Significance of difference between population means for the control group and experimental group were determined by an unpaired Student's t test. Correlation coefficients were determined by linear regression analysis.

RESULTS

Delipidation of LDL. LDL was solubilized with NaDOC as described (*19*), and samples containing apoB100 were separated from lipid micelles by two sequential gel filtration chromatography steps. The resulting aqueous soluble preparation was designated apoB100−TG complex since it contained no detectable amounts of detergent, phospholipid, cholesterol, or CE, but retained ∼70% of the native LDL TG (Table 1). In total, apoB−TG was prepared from 25

Table 1: Molar Lipid Composition (mol/mol apoB100) of Native and Reconstituted Lipoprotein Particles

complex	phospholipid intial[a]	phospholipid final[b]	cholesterol	cholesteryl ester	triacylglycerol
native LDL	509 ± 25		750 ± 28	634 ± 24	367 ± 26
apoB100−TG					242 ± 6
100-POPC−apoB100	100	75 ± 4			242 ± 8
300-POPC−apoB100	300	265 ± 5			242 ± 9

[a] Phospholipid content before reisolation on a Superose-6 gel filtration column. [b] Phospholipid content after reisolation on a Superose-6 gel filtration column ± SD.

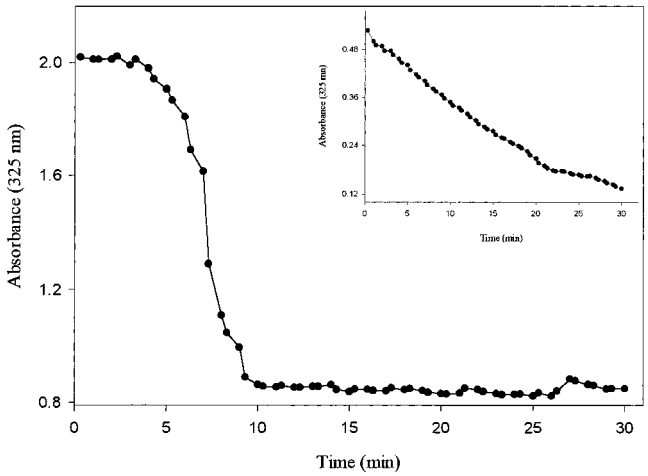

FIGURE 1: Kinetics of POPC association with apoB100. The reduction in turbidity (absorbance at 325 nm) at 10 °C of POPC vesicles (1 mg/mL Tris buffer) after the addition of apoB100−TG (0.25 mg of protein) is shown. The inset shows the reduction in turbidity at 24 °C of DMPC vesicles (1 mg/mL) in Tris buffer after addition of apoA-I (0.25 mg of protein).

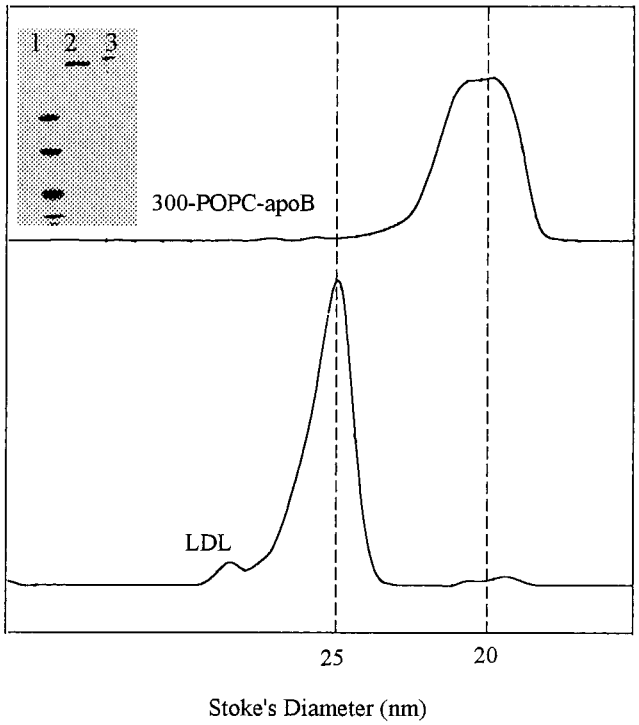

FIGURE 2: Determination of size and homogeneity of reconstituted LDL. Densitometer profiles of reconstituted LDL particles (300-POPC−apoB) and native LDL (LDL) subjected to nondenaturing electrophoresis on 4−15% gradient acrylamide gels are shown. Estimated hydrodynamic diameters were determined from reference standards as described in Experimental Procedures. The inset shows the actual acrylamide gel, where lane 1 corresponds to molecular weight standards (17.0 nm thyroglobulin, 12.2 nm ferritin, 10.4 nm catalase, 8.2 nm lactate dehydrogenase, and 7.1 nm albumin), lane 2 reconstituted LDL, and lane 3 native LDL.

individual subjects with LDL that differed in lipid composition. The mean w/w percent composition of the starting LDL was 18% TG, 21% phospholipid, 15% free cholesterol, 18% cholesteryl esters, and 28% protein (Table 1). The absolute amount of TG that was recovered with the apoB in individual preparations largely reflected the TG content of the starting LDL. Analysis of apoB100 in the apoB100−TG complex by SDS−polyacrylamide gel electrophoresis showed an intact apoB100 polypeptide with an apparent molecular mass of approximately 500 000 Da (data not shown). The possibility of aggregation of the apoB100−TG complexes was tested by non-denaturing gel electrophoresis. ApoB100−TG was found to migrate into the gradient gel and exhibited a single discrete band with a diameter of 18 nm (data not shown). These data suggest that apoB100 is able to solubilize a significant amount of TG in the absence of other lipids, and association of TG with apoB100 not only renders solubility in aqueous solutions but also maintains structural integrity and prevents self-aggregation.

Association of ApoB100−TG with POPC and DMPC. The apoB100−TG complex was combined with various amounts of POPC vesicles, and the kinetics of association was monitored by determining the reduction in turbidity at 325 nm. As illustrated in Figure 1, apoB100−TG was able to rapidly (within 10 min) solubilize POPC vesicles in a spontaneous manner at various temperatures tested, above or below the transition temperature of POPC. A total reaction time of 30 min yielded a sigmoidal-shaped curve, with a constant initial absorbance followed by a rapid decrease in absorbance at 10 min and then a plateau with no further change in absorbance. Similar results were obtained when DMPC was substituted for POPC (data not shown). The rapid and spontaneous association of the apoB100−TG complex with phospholipid vesicles was in sharp contrast to the slow and gradual association of apoA-I with DMPC yielding an exponential clearance curve with first-order kinetics (Figure 1, inset). Similar to previous studies (*20*), apoA-I did not interact with POPC vesicles under the same conditions (data not shown). Examination of the apoB100−PC particle size by gradient gel (4−15%) electrophoresis under nondenaturing conditions showed that the apoB100−PC particles (re-isolated by Superose-6 gel filtration chromatography) exhibit a single discrete band of 20 nm (Figure 2).

Characterization of Secondary Structure and Stability of ApoB100. The far-UV CD spectra for native LDL, apoB100−TG, and apoB100−PC all showed a shallow negative trough between 210 and 220 nm (Figure 3 and Table 2), indicating

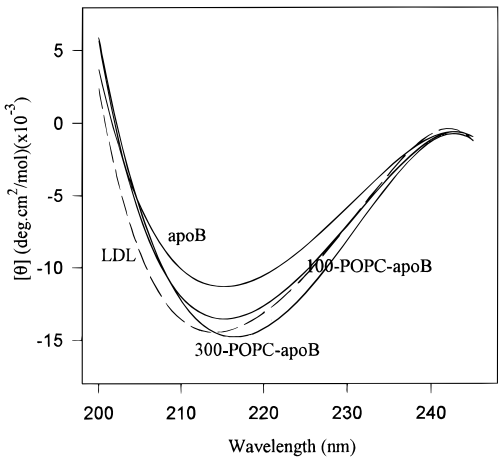

FIGURE 3: Circular dichroic spectra of apoB100 on different reconstituted LDL particles. The spectra of apoB100 on native LDL (dashed line) were recorded from 260 to 200 nm with a Jasco 41A spectropolarimeter and are shown relative to the spectra for apoB100−TG and reconstituted LDL particles containing 300 and 100 molecules of POPC (solid lines).

Table 2: Secondary Structure and Stability of ApoB100 in Lipoprotein Complexes

complex	$D_{1/2}$[a] (M GdnHCl)	α-helix (%)[b]
native LDL	2.52	49.1
apoB100−TG	2.89	17.0
100-POPC−apoB100	2.59	27.5
300-POPC−apoB100	2.11	34.2

[a] Midpoint of GdnHCl denaturation ± 0.03 M (SD). [b] α-Helix content determined from molar ellipticities at 222 nm ± 4% (SD).

that apoB100 contains a small but significant amount of α-helical structure. The addition of ∼300 molecules of POPC to apoB100−TG increased the amount of α-helix in apoB100 and yielded a spectrum that is very similar to that for native LDL, suggesting that much of the secondary structure of apoB100 is similar on the two lipoprotein samples. These data are also consistent with previous studies (*21*) showing that apoB100 undergoes a structural change when complexed with lipid, wherein its α-helical content increases. The general features of the CD spectra of apoB100−TG complex and the two apoB100−PC preparations were similar to those observed for native LDL, except for a slight rightward shift in spectra for the delipidated and the reconstituted particles. This leftward shift in spectra for LDL may be due to the contributions of cholesterol and CE to the region below 220 nm (*22*). These lipids were absent in the delipidated and the phospholipid particles.

Results of isothermal denaturation of native LDL and apoB100−lipid complexes are shown in Figure 4. In the presence of GdnHCl, apoB100 on native LDL underwent a gradual unfolding, but it appeared to be resistant to complete denaturation. The protein exhibited a complex 3−4 state unfolding profile and had at least two partially stable intermediates. At the highest concentration of GdnHCl (5.8 M), LDL−apoB100 retained much of its secondary structure and still had approximately 85% of its amphipathic α-helixes. ApoB100 in the delipidated apoB−TG complex unfolded in a manner that paralleled the curve obtained for LDL−apoB100, but commencing and terminating at a much lower α-helical content. Unlike that of LDL−apoB100, the α-helixes of apoB100 in apoB−TG complex were completely unfolded and in random coil at 5.8 M GdnHCl. Phospholipidation of the apoB100−TG complex appeared to stabilize apoB100 secondary structure and protect apoB100 from denaturation by GdnHCl. The addition of increasing amounts of POPC to apoB100−TG gradually increased the overall α-helical content of apoB100 and decreased the effectiveness of GdnHCl in unfolding apoB100. Therefore, the secondary structure and stability of apoB100 is sensitive to the amount of phospholipid bound.

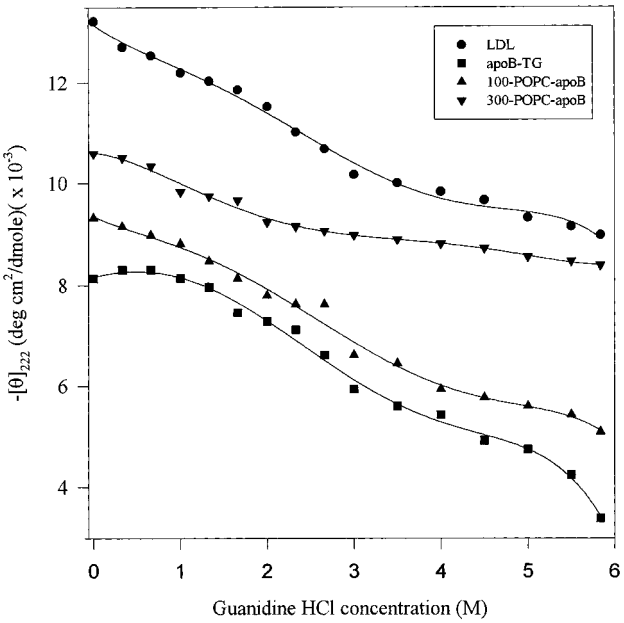

FIGURE 4: Effect of GdnHCl concentration on the molar ellipticity at 222 nm for LDL and reconstituted LDL. Aliquots of each sample (33.3 μg of protein/mL) were preincubated with 0−6 M GdnHCl in 0.05 M phosphate buffer for 72 h at 4 °C. The molar ellipticity at 222 nm was determined for LDL, apoB100, and reconstituted LDL particles containing 100 and 300 molecules of POPC. Values are the average of duplicate determinations.

Table 3: Electrophoretic Characteristics of Native and Reconstituted Lipoprotein Particles

complex	mobility[a] (μm s⁻¹ cm V⁻¹)	surface potential[b] (mV)	charge density[c] (×10² esu/cm²)	valence[d] (e)
native LDL	−0.311	−6.0	−6.48	−82.1
apoB100−TG	−0.150	−2.9	−3.12	−39.5
100-POPC−apoB100	−0.185	−3.6	−3.85	−48.8
300-POPC−apoB100	−0.251	−4.9	−5.22	−66.2

[a] Corrected electrophoretic mobility (0.5% agarose) ± 0.01 (SD). [b] Charge potential at the particle surface ± 0.2 (SD). [c] Net density of surface charge ± 0.02 × 10² (SD). esu, electrostatic units. [d] The number of excess negative charges in electronic units ± 0.1 (SD).

Characterization of Net Charge of ApoB100. Electrokinetic properties of native LDL, apoB100−TG, and apoB100−PC were determined by agarose gel electrophoresis (Table 3). On agarose gels, LDL exhibited a distinct band that migrated into a region of β-mobility with a surface potential of −6 mV. The lipid-poor apoB100−TG complex exhibited a band located near the origin of the gel with a surface potential of −2.9 mV. Addition of increasing amounts of POPC to apoB100−TG resulted in a gradual increase in the electrophoretic mobility which corresponded to the increased charge density and valence. The apoB100−TG complex had a lower charge density relative to apoB100−PC and native LDL. Therefore, addition of phospholipids restored apoB100

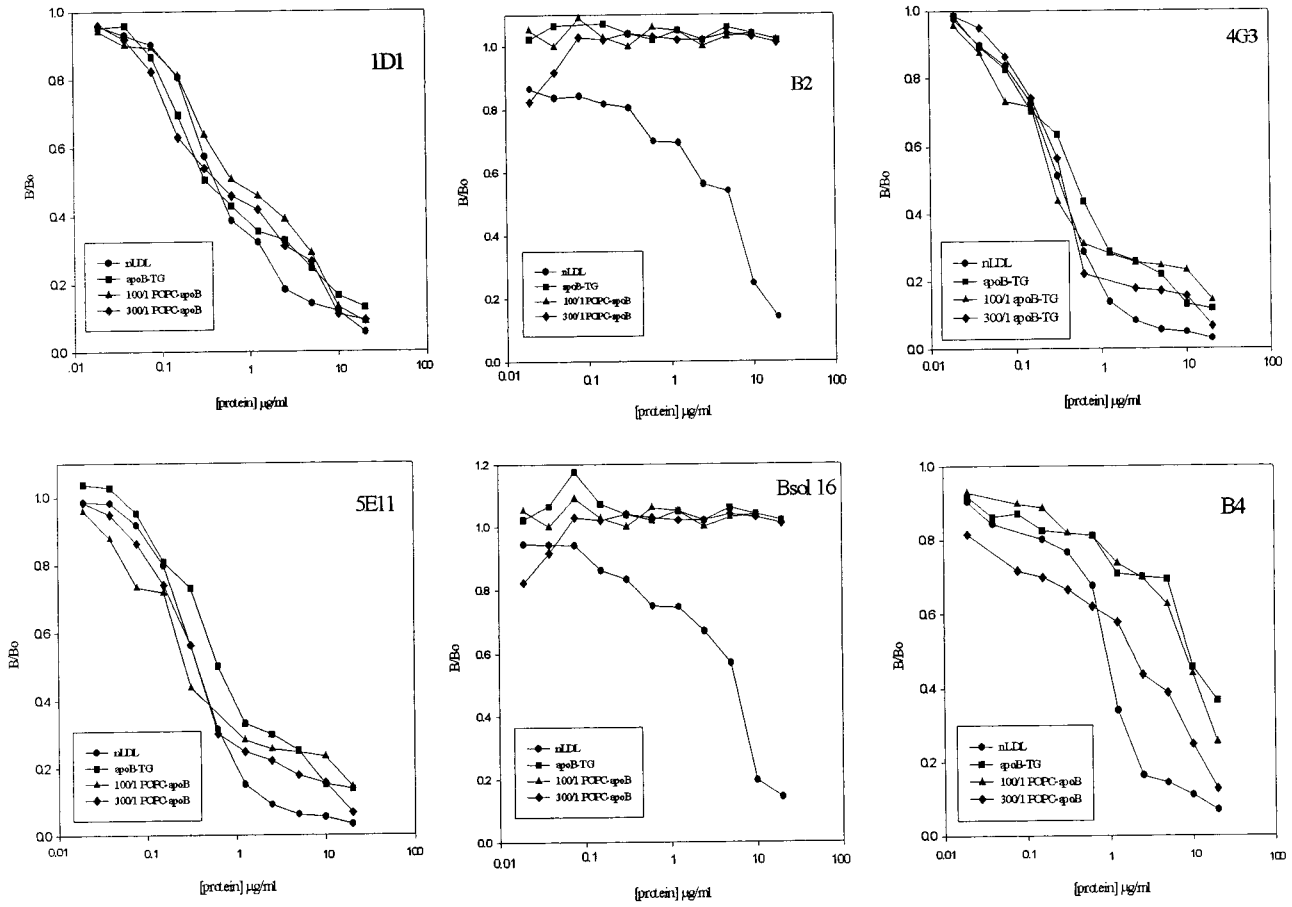

FIGURE 5: Competitive radioimmunometric assay of apoB100−TG, phospholipid-associated apoB100, and native LDL. A panel of anti-apoB100 mAbs were appropriately diluted and incubated overnight with dilutions of apoB100−TG, phospholipid-associated apoB100 native LDL in LDL-coated microtiter wells, as indicated in Experimental Procedures. Bound anti-apoB mAb was detected with ^{125}I-anti-mouse IgG. Competition curves for certain representative mAbs are shown. B/B_o represents radioactivity bound in the presence of competitor as a fraction of that bound in the absence of competitor.

conformation such that approximately 81% of electrokinetic properties of LDL−apoB100 has been recovered.

Immunoreactivity of ApoB100 with Monoclonal Antibodies. Immunoreactivities of apoB100−TG complexes and phospholipid-associated apoB100−TG were examined in a competitive solid-phase radioimmunometric assay, with a panel of 28 anti-apoB mAbs specific for epitopes that range from the amino terminus to the carboxy terminus of apoB100. A representative selection of competition curves is shown in Figure 5. While apoB100−TG and phospholipid-associated apoB100 competed effectively with immobilized native LDL for binding to certain mAbs (1D1 and 5E11), other mAbs were less effective competitors (B4) or were unable to compete with the native LDL (B2). The ED_{50} values for all mAbs are presented in Table 4. Whereas all 28 antibodies displayed strong immunoreactivity toward native LDL, apoB100−TG and phosholipid-associated apoB100 showed variable reactivity to the different antibodies. For certain of the mAbs (e.g., 1D1, 4G3, and 5E11) the ED_{50}s for apoB100−TG were similar to native LDL. For other mAbs (e.g., B2, Bsol 6, and 2G4), even the highest concentration of apoB100−TG that was tested failed to compete with the immobilized LDL. Interestingly, for certain epitopes that were partially expressed on apoB100−TG (Bsol 3, B4, and MB47), addition of phospholipids resulted in an increase in immunoreactivity such that the ED_{50} values of phospholipid-associated apoB100 were similar to those of native LDL. Thus, partial delipidation of LDL brought about major conformational changes to specific regions of apoB100. These conformational changes either masked or changed specific apoB100 epitopes. In only some cases could the addition of phospholipids to apoB−TG fully restore the immunoreactivity to that of native LDL−apoB100.

Binding of ApoB100−TG, ApoB100−PC, and Native LDL to the LDL Receptor. Whereas native LDL could efficiently compete with ^{125}I-LDL for binding to the LDL receptor on cultured human fibroblasts, neither apoB100−TG nor apoB100−PL was an effective competitor, even when tested at high concentration (results not shown).

DISCUSSION

The structural organization of apoB100, complexed with TG, was probed with a panel of mAbs that had been raised against either native LDL or delipidated, resolubilized apoB. The results in Table 4 show that epitope expression in apoB100−TG is largely independent of the physical form of the apoB that was used as the immunogen to generate the mAbs, but rather reflects intrinsic features of apoB100 structure. As can be seen in Figure 6A, immunoreactive epitopes in apoB100−TG are nonequally distributed in apoB primary structure. Epitopes situated between residues 2148 and 2543 or in the carboxy-terminal 500 amino acids of apoB

Table 4: Immunoreactivity of Various Monoclonal Antibodies to ApoB100[a]

monoclonal antibody	epitope	ED_{50} native LDL (μg/mL)	ED_{50} apoB (μg/mL)	ED_{50} 100/1-apoB−POPC (μg/mL)	ED_{50} 300/1-apoB−POPC (μg/mL)
$B_{sol}12$[b]	1−70	2.21	>20	>20	>20
$B_{sol}3$[b]	186−670	0.73	1.44	2.20	0.92
$B_{sol}10$[b]	186−670	2.20	11.2	8.30	9.01
$B_{sol}14$[b]	186−670	1.46	22.1	15.4	6.20
1D1	474−539	0.64	0.57	0.95	0.65
746	474−539	2.71	>20	>20	>20
3E11	995−1328	16.2	>20	>20	>20
374	1305−1542	0.56	5.67	3.12	8.62
1C4	1694−1880	0.29	10.4	6.20	3.99
2D8	1438−1481	1.20	0.73	0.96	0.72
B4	1854−1878	0.83	8.10	7.82	1.82
3A5	1881−2100	1.52	8.42	7.40	13.4
2G4	2148−2375	3.22	>20	>20	>20
B2	2239−2331	7.21	>20	>20	>20
$B_{sol}6$[b]	2488−2543	0.72	>20	>20	>20
278	2658−3249	0.38	1.34	0.42	0.51
3G9	2658−3249	1.06	1.78	1.15	1.43
3F5	2835−2922	0.82	1.32	1.44	3.20
4G3	2980−3084	0.43	0.63	0.43	0.57
Mb47	3441−3569	0.82	7.34	6.01	3.42
5E11	3441−3569	0.43	0.62	0.43	0.57
588	3441−3687	1.85	>20	>20	>20
MB43	4027−4081	0.84	>20	>20	>20
$B_{sol}16$[b]	4154−4189	6.31	>20	>20	>20
234	4235−4536	2.42	>20	>20	>20
4H11	4235−4536	1.85	>20	>20	>20
605	4235−4536	0.82	>20	>20	>20
$B_{sol}7$[b]	4521−4536	15.2	>20	>20	>20

[a] The antibodies were raised against either delipidated LDL or native LDL. [b] Antibodies raised against delipidated LDL.

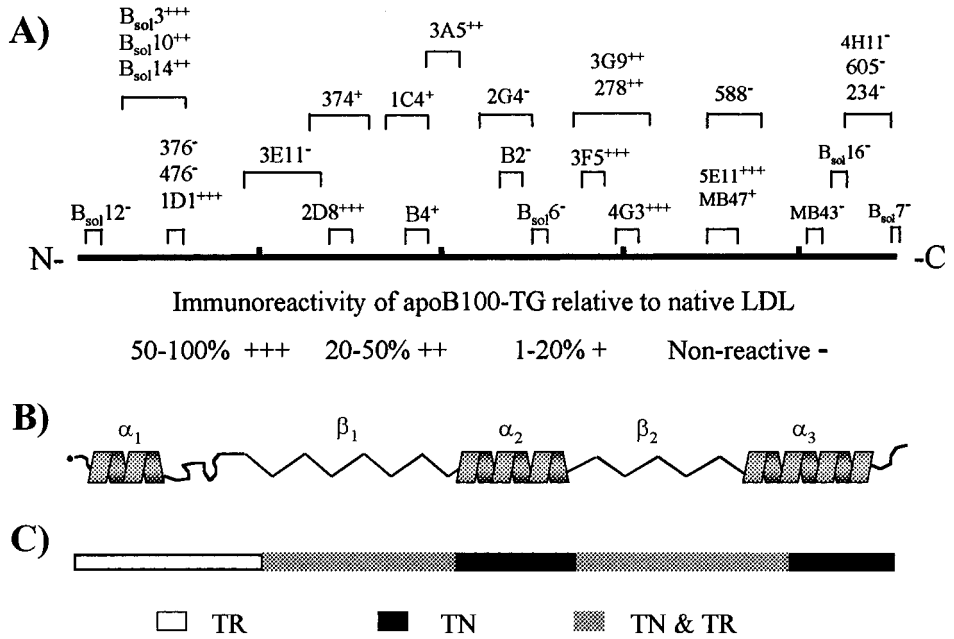

FIGURE 6: Relative immunoreactivity of apoB epitopes in apoB100−TG as a function of their position in apoB primary and predicted apoB secondary structure. (A) The relative immunoreactivity of apoB epitopes is based on the data presented in Table 4. Mapping of apoB epitopes within apoB primary structure has been previously described (*17*). (B) A representation of the pentapartite model of apoB secondary structure as described by Segrest et al. (*6*). (C) Distribution of trypsin-releasable and trypsin-nonreleasable peptides in apoB primary structure (*5*, *6*).

were not expressed in apoB100−TG. Yang et al. (*5*) have shown that both of these segments of the apoB polypeptide are intimately associated with lipid and/or are not accessible to trypsin in native LDL (Figure 6C). Moreover, in the pentapartite model of apoB secondary structure, as proposed by Segrest and al. (*6*) (Figure 6B), these two regions comprise the α_2 and α_3 domains that are predicted to contain dense clusters of amphipathic α-helixes that have a high affinity for lipid. In contrast to epitopes in the α_2 and α_3 domains, most epitopes situated elsewhere in apoB retained partial or complete immunoreactivity in apoB100−TG. This includes 4 of 6 epitopes that have been mapped to the amino terminus of apoB primary structure, a region that is thought to adopt a globular structure with relatively low affinity for lipid and to include a cluster of amphipathic α-helixes (*5*, *6*). Likewise, 11 of 13 epitopes that were situated in regions

predicted to adopt an amphipathic β-structure (β_1: 827−1961, and β_2: 2611−3867) (*6*) with a relatively high affinity for lipid (*5*) retained partial or total immunoreactivity in apoB100−TG compared to native LDL. Thus, complexed with TG, the conformational integrity of LDL−apoB100 has, to some extent, been preserved as determined by structural and immunoreactive properties. Moreover, the relative reactivity of epitopes in apoB100−TG appears to correlate with the putative domain structures that have been predicted for apoB in native lipoproteins (*5*, *6*).

The kinetics of phospholipid association was determined, and it was found that unlike apoA-I, apoB100−TG was able to spontaneously and rapidly interact with both POPC and DMPC. While apoB100−TG contains a small amount of α-helical structure that is completely denatured by GdnHCl, association with POPC results in a progressive increase in its α-helical content (Table 2) and a significantly reduced propensity to be denatured (Figure 4). Thus, the α-helical segments of lipidated apoB100 may be involved in interactions with phospholipids. The stabilizing effect of POPC suggests that the α-helical structure may also be critical to the integrity of apoB100. Both the predicted secondary structure and circular dichroic measurements suggest that apoB100 may contain up to 40−50% α-helical structure (*1*, *23*). This is consistent with what has been observed with the exchangeable apoproteins; amphipathic α-helixes are thought to be important for phospholipid binding and lipoprotein stability (*6*, *11*). In contrast, other studies have suggested that the β-sheet structure of apoB100 is critical to lipid binding and structural stability of apoB100 (*4*, *5*). Our results suggest that the non-α-helical structure in apoB100 may stabilize the highly hydrophobic domains by governing interactions with neutral lipids, while the α-helixes of apoB100 probably facilitate phospholipid binding and the structural stabilization of the lipoprotein. Taken together, the data suggest that both the α-helical and β-strand structure of apoB100 act in concert to allow for a certain amount of conformational plasticity and yet maintain the lipoprotein structural integrity.

Phospholipidated apoB100 is protected from complete denaturation and undergoes only a partial unfolding of α-helixes (Figure 4). The data are consistent with a multiphase denaturation, wherein the protein undergoes a stepwise denaturation of unique domains in apoB100 that are progressively exposed as the molecule loses organized structure. The observation that only 5−15% of the α-helical structure of the POPC-bound apoB100 can be unfolded by GdnHCl suggests that denaturation does not result in the complete dissociation of apoB100 from the lipid interface but represents the unfolding of specific exposed domains of apoB100 on the lipoprotein surface. It would appear that the highly helical conformation of POPC-bound apoB100 shields the peptide backbone and aromatic residues of the protein from guanidinium ions. This reduction in GdnHCl binding sites may be partially due to apoB100 being tightly interwoven within the POPC environment. This may result in the protection of aromatic residues, buried deeply within the hydrophobic environment of the α-helical segments of apoB100. In contrast, apoB100−TG not associated with POPC appears to have more exposed aromatic residues and peptide bonds and yields a less stable apoB100 that is more easily accessible to GdnHCl and prone to complete denaturation.

Complexation of apoB100−TG with POPC appears to disrupt the interactions between apoB100 and TG and leads to an increased exposure of unique, negatively charged domains within apoB100. Electrokinetic analysis of apoB100−TG and POPC-bound apoB100 showed that the addition of POPC increased net negative charge on apoB100 by increasing the molecular valence. Our results further show that a relationship exists between apoB100 surface charge, α-helical content, and stability for the different apoB100-containing particles (Table 2). An increase in the magnitude of the negative surface potential on POPC-bound apoB100 appears to be directly related to an increase in α-helix content and reduced propensity to be denatured.

Addition of phospholipids to apoB100−TG complexes caused a partial or complete recovery of the expression of certain of the epitopes in the putative α_1, β_1, and β_2 domains of apoB ($B_{sol}3$, $B_{sol}14$, 1C4, B4, 278, and MB47) that were not fully reactive in apoB100−TG. In contrast, addition of POPC to the apoB100−TG failed to restore expression of epitopes in the α_2 and α_3 domains, despite the normalization of the α-helical content of the complexes as monitored by circular dichroic spectroscopy. Thus, the recovery of immunoreactivity of certain epitopes may result from regeneration of α-helical structure in the α_1 domain and, potentially also, within domains thought to have a predominantly β-strand structure. However, normalization of α-helical content is not sufficient for the expression of epitopes in the α_2 and α_3 domains.

Our data suggest that apoB100−TG is a metastable "transition particle" that contains an unstable organization. Intercalation of phospholipids causes the reorganization of the complex and promotes the formation of a condensed and stabilized lipoprotein particle. The condensation of the particle appears to bring newly exposed negatively charged residues on apoB100 into closer proximity. This may define unique charged domains in the apoB100 molecule, domains that have specific metabolic functions. Triglycerides clearly play a role in determining the conformation of apoB100. We have shown here that several mAbs in the β_1 (2D8) and β_2 (3F5, 4G3, and 5E11) domains are fully expressed in apoB100−TG, whereas we have previously reported that these same epitopes are not immunoreactive in completely delipidated and resolubilized apoB (*16*). The retention of TG by deoxycholate-delipidated apoB and the apparent role of TG in maintaining the expression of epitopes in the β_1 and β_2 domains may indicate that, in native LDL, these regions may be intimately bound to core lipids, an association that may normalize the conformation of the β-strands. Thus, the epitopes that we monitor could be composed of amphipathic β-strands or these latter could serve as a scaffold for the appropriate presentation of the epitopes. Interestingly, it has been proposed that the β_1 and β_2 domains represent irreversible lipid-binding regions of apoB (*6*). Our results support this hypothesis, and we furthermore propose that the β_1 and β_2 domains not only tightly bind neutral lipid but also represent relatively inflexible regions of apoB structure that could act as a backbone during lipoprotein assembly. On the other hand, the lack of expression of epitopes in the α_2 and α_3 domains indicates that the conformation of these regions is highly dependent on the physical and chemical properties of the lipoprotein particle. These amphipathic α-helical domains may, therefore, represent flexible lipid-

binding regions that allow the particles to accommodate varying amounts of lipid during lipoprotein assembly and intravascular metabolism. In support of this latter hypothesis, we have recently observed that epitopes in the α_3 domain are particularly sensitive to changes in native LDL particle diameter (X. Wang and R. W. Milne, manscript in preparation).

ACKNOWLEDGMENT

We thank Drs. Zemin Yao and Yves Marcel for stimulating discussion and a critical evaluation of the manuscript and Tracey Neville for expert technical assistance. Monoclonal antibodies MB43 and MB47 were kindly provided by Drs. Steven Young, Linda Curtiss, and Joseph Witztum and monoclonal antibodies B2 and B4 by Professor Jean-Charles Fruchart.

REFERENCES

1. Chan, L. (1992) *J. Biol. Chem. 267*, 25621−25624.
2. Chatteron, J. E., Phillips, M. L., Curtiss, L. K., Milne, R. W., Marcel, Y. L., and Schumaker, V. N. (1991) *J. Biol. Chem. 266*, 5955−5962.
3. Chatterton, J. E., Phillips, M. L., Curtiss, L. K., Milne, R., Fruchart, J. C., and Schumaker, V. N. (1995) *J. Lipid Res. 36*, 2027−2037.
4. Chen, G. C., Hardman, D. A., Hamilton, R. L., Mendel, C. M., Schilling, J. W., Zhu, S., Lau, K., Wong, J. S., and Kane, J. P. (1989) *Biochemistry 28*, 2477−2484.
5. Yang, C., Gu, Z., Weng, S., Kim, T. W., Chen, S., Pownall, H. J., Sharp, P. M., Liu, S., Li, W., Gotto, A. M., Chan, L. (1989) *Arteriosclerosis 9*, 96−108.
6. Segrest, J. P., Jones, M. K., Mishra, K. V., Anatharamiaah, G. M., Garber, D. W. (1994) *Arterioscler. Thromb. 14*, 1674−1685.
7. McLeod, R. S., Wang, Y., Wang, S., Rusiñol, A., Links, P., and Yao, Z. (1996) *J. Biol. Chem. 271*, 18445−18455.
8. Schumaker, V. N., Phillips, M. L., and Chatterton, J. E. (1986) *Adv. Protein Chem. 45*, 205−235.
9. Helenius, A., and Simons, K. (1971) *Biochemistry 10*, 2542−2547.
10. Williams, P. T., Krauss, R. M., Nichols, A. V., Vranizan, K. M., and Wood, P. D. (1990) *J. Lipid Res. 31*, 1131−1140.
11. Sparks, D. L., and Phillip, M. C. (1992) *J. Lipid Res. 33*, 123−130.
12. Sokoloff, L. (1974) *Proc. Soc. Exp. Biol. Med. 146*, 1166−1172.
13. Markwell, M. K., Hass, S. M., Bieber, L. L., and Tolbert, N. E. (1978) *Anal. Biochem. 87*, 206−210.
14. Chen, G. C., and Kane, J. P. (1986) *Methods Enzymol. 128*, 519−527.
15. Milne, R. W., Theolis, R., and Verdery, R. B. (1983) *Arteriosclerosis 3*, 23−30.
16. Marcel, Y. L., Hogue, M., Weech, P. K., and Milne, R. W. (1984) *J. Biol. Chem. 259*, 6952−6957.
17. Pease, R. J., Milne, R. W., Jessup, W. K., Law, A., Provost, P., Fruchart, J. C., Dean, R. T., Marcel, Y. L., and Scott, J. (1990) *J. Biol. Chem. 265*, 553−564.
18. Bilheimer, D. W., Eisenberg, S., and Levy, R. I. (1972) *Biochim. Biophys. Acta 260*, 212−221.
19. Lundberg, B. O., and Suoiminen, L. (1984) *J. Lipid Res. 25*, 550−558.
20. Massey, B. J., Gotto, A. M., and Pownall, H. J. (1981) *Biochemistry 20*, 6630−6635.
21. Ginsburg, G. S., Small, D. M., and Atkinson, D. (1982) *J. Biol. Chem. 257*, 8216−8227.
22. Walsh, M. T., and Atkinson, D. (1983) *Biochemistry 22*, 3170−3178.
23. Kane, J. P. (1983) *Annu. Rev. Physiol. 45*, 637−645.

BI9718853